**Supplement Material.**

## Materials and methods

### Animals

Mice were weaned at 4 weeks of age and maintained on a standard rodent chow diet (Diet #5015; Harlan Teklad, Madison, WI). At 8 weeks of age, mice were fasted for 12 hours, weighed, bled by retro-orbital puncture and transferred onto a high cholesterol diet (15.8% fat, 1.25% cholesterol, 7.5% casein without sodium cholate: Diet #94059; Harlan Teklad, Madison, WI). Following diet intervention, mice were fasted for 12 hours, weighed and bled by retro-orbital puncture for lipid analyses.

### Bone marrow transplantation

To distinguish donor from recipient bone marrow (BM)-derived cells and accurately monitor hematopoietic reconstitution in transplanted mice, we derived 2 colonies of C57BL/6J (N10) LDLR-/-G2A+/+ and LDLR-/-G2A-/- mice, one carrying the original C57BL/6J-associated hematopoietic Ly5.2 (CD45.2) alloantigen, the other carrying the differential Ly5.1 (CD45.1) alloantigen derived from the B6.SJL-Ptprc$^{a}$ Pep3$^{b}$/BoyJ strain of C57BL/6J mice (Jackson Laboratories). Subsequently, chimeric LDLR-/- mice were generated in which G2A deficiency or G2A expression is limited to BM-derived cells or non-BM derived cells (resident tissues) by reciprocal BM transplantation (BMT) of Ly5.1 LDLR-/-G2A+/+ and Ly5.1 LDLR-/-G2A-/- mice with congenic Ly5.2 LDLR-/-G2A+/+ or Ly5.2 LDLR-/-G2A-/- BM cells (producing 4 groups of chimeric LDLR-/- mice). LDLR-/-G2A+/+ Ly5.1 and LDLR-/-G2A-/- Ly5.1 recipients were lethally irradiated (2

doses of 450 RADS ionizing radiation spaced by 3 hours) and transplanted at 6 weeks of age with $5x10^6$ BM mononuclear cells from LDLR-/-G2A+/+ Ly5.2 or LDLR-/-G2A-/- Ly5.2 donor mice. Six weeks following BMT, blood samples were collected and processed for flow cytometric analysis of reconstitution of major hematopoietic lineages (CD11b, CD4, CD8, CD19). Successfully reconstituted mice were transferred onto a high-cholesterol diet (Diet #94059; Harlan Teklad, Madison, WI) for 20 weeks. Blood samples collected following diet intervention were also analyzed by flow cytometry to confirm stable reconstitution of major hematopoietic lineages. The origin of lesional macrophages from donor bone marrow (Ly5.2) was confirmed by co-immunofluorescence staining of aortic cryosections as previously described {Parks, 2006 #820} with the following antibodies: Mouse anti-Ly5.1$^{BIOTIN}$ (Southern Biotechnology) + Rat anti-CD11b (BD Pharmingen) followed by Streptavidin$^{ALEXA488}$ (Molecular Probes) + Goat anti-Rat IgG$^{ALEXA555}$ (Molecular Probes), and Mouse anti-Ly5.2$^{BIOTIN}$ (Southern Biotechnology) + Rat anti-CD11b (BD Pharmingen) followed by Streptavidin$^{ALEXA488}$ + Goat anti-Rat IgG$^{ALEXA555}$.

**Measurement of lipoprotein profiles and FPLC**

Plasma samples were processed for measurement of total cholesterol, unesterified cholesterol, HDL cholesterol, LDL-cholesterol, triglycerides and free fatty acids by enzymatic procedures as previously described (1, 2). LDL-cholesterol concentrations obtained using this method includes both VLDL and LDL fractions. Online cholesterol analysis of plasma lipoproteins by FPLC (CLIP) was performed as described by Garber and colleagues (3). Profiles were decomposed into component peaks and analyzed for

relative area using PeakFit (SPSS Science, Chicago, IL). To prepare plasma HDL fractions for immunoblot analysis of apolipoprotein composition, plasma was fractionated using a HiLoad 16/60 Superdex 200 prep grade column (Amersham Biosciences) or a Superose 6 10/300 GL column (Amersham Biosciences) on a Biologic DuoFlow FPLC system (Bio-Rad). Plasma (200μl) was injected onto the column and separated with PBS containing 0.02% sodium azide at a flow rate of 1 ml/minute. 0.5ml fractions were collected and analyzed for total cholesterol content utilizing enzymatic cholesterol reagents (Thermo Electron Corporation).

**SDS-polyacrylamide gel electrophoresis and immunoblotting**

FPLC fractions, 10μl diluted plasma (1:100), hepatocyte culture supernatants, or cell lysates were combined with an equal volume of SDS-PAGE reducing sample buffer and separated on 12% acrylamide/bis-tris gels. Proteins were transferred to Immobilon-P membranes (Millipore) and blocked with PBS containing 0.05% Tween-20 and 5% non-fat milk, incubated with primary antibodies, washed in blocking buffer, and incubated with horseradish peroxidase-conjugated secondary antibodies. Immunoreactive proteins were visualized using enhanced chemiluminescence (Immun-star; Bio-Rad). Antibodies used were as follows: Rabbit anti-ApoA1 (Biodesign), rabbit anti-ApoE (Biodesign), rabbit anti-ABCA1 (Novus Biologicals), anti-ERK2 (Santa Cruz Biotechnology) and rabbit anti-G2A (generously provided by Dr. Owen Witte). Immunoreactive proteins were quantified by densitometric scanning using Scanalytic's One-Dscan version 1.31.

**Hepatocyte isolation**

Mice were anesthetized using a ketamine/xylazine mixture (150mg/15mg per Kg body weight) and the superior vena cava was clamped with a micro vascular clamp. The inferior vena cava was immediately cannulated with a 25-gauge winged infusion needle and the hepatic portal vein was severed. The liver was perfused with 30ml of $Ca^{2+}$/$Mg^{2+}$-free Hank's Balanced Salt Solution (HBSS) containing 0.2mM EDTA and 20mM glucose at a constant rate of 4ml/min using a syringe pump. The liver was then perfused with 30ml of $Ca^{2+}$/$Mg^{2+}$-containing HBSS with 20mM glucose and 100U/ml collagenase type I (Sigma) at a rate of 4ml/min. The liver was removed and placed into a culture dish containing 20ml of ice-cold William's medium E (Invitrogen) containing 0.1% BSA, L-glutamine (2mM), penicillin (100U/ml), streptomycin sulfate (100µg/ml), and fungizone (250ng/ml; Omega Scientific). The liver was gently teased apart and subsequently passed through a 100µm strainer. Hepatocytes were obtained by gravity sedimentation (15 minutes) followed by 2 washes in Williams medium (50g for 3 minutes at 4°C). Hepatocytes were resuspended in 20ml of Williams medium, counted and assessed for viability using trypan blue exclusion. The yield of hepatocytes averaged from 20-40x$10^6$ from each liver and viability was consistently greater than 90%.

**Quantitative real-time PCR**

Freshly prepared hepatocytes or thioglycolate-elicited peritoneal macrophages were lysed in RNA lysis buffer and processed for RNA extraction using the absolutely RNA miniprep kit (Stratagene). RNA concentrations and RNA quality (28S:18S ribosomal

RNA ratio) were measured using the Experion automated microfluidics electrophoresis system (BioRad) with preformed RNA standards for single-platform RNA detection and data analysis. 100ng of each RNA sample was used to synthesize cDNA using the iScript cDNA synthesis kit (BioRad). All primers were tested under a range of annealing temperatures (54°C – 62°C) and cDNA dilutions (1:10, 1:100 and 1:1000) to ensure optimum product amplification and comparable PCR efficiency between housekeeping gene (G3PDH)-specific primers and target gene-specific primers. Each cDNA was subsequently diluted 1:10 and 2μl of this dilution used in the PCR reaction (20μl) that contained reagents from the iQ SYBR Green Supermix (BioRad). In every experiment, each PCR reaction was performed in triplicate and run on an iCycler iQ Multicolor Real-time PCR detection system (BioRad). PCR conditions were: 95°C 3 minutes, 95°C 10 seconds, followed by 40 cycles at 95°C for 15 seconds, 58°C for 1 minute, 72°C for 30 seconds, and finally 95°C for 1 minute. Data showing G2A expression (Figure 2C) were analyzed using the relative expression method: Relative expression = $2^{-(S\Delta CT-C\Delta CT)}$ where ΔCT is the average difference in cycle threshold (CT) between G2A and the housekeeping gene, G3PDH, in hepatocytes (S) and macrophages (C). Data in figure 3B were analyzed using the relative expression method: Relative expression = $2^{-(S\Delta CT-C\Delta CT)}$ where ΔCT is the average difference in cycle threshold (CT) between the gene of interest and G3PDH in G2A-/- (S) and G2A+/+ (C) cells. Forward (F) and reverse (R) primers were as follows: G3PDH F: GCCTCAACTATATGGTCTAC, G3PDH R: CCATCTTCCAGGAGTGAG. G2A F: GCCACCATGAGATCAGAACC, G2A R: CACCACCACCAGGACCAC. ApoE F: TGCTGTTGGTCACATTGC, ApoE R: CAGTGCCGTCAGTTCTTG. ApoA1 F: TTCGCTAATGTGTATGTG, ApoA1 R:

TCTTTCTCCAGGTTATCC. ABCA1 F: TACCCACCCTACGAACAAC, ABCA1 R: TGAGAACAGGCGAGACAC. ABCG5 F: TGTCCTACAGCGTCAGCACC, ABCG5 R: GGCCACTCTCGATGTACAAGG. ABCG8 F: GACAGCTTCACAGCCCACAA, ABCG8 R: GCCTGAAGATGTCAGAGCGA. SRB1 F: GCAAATTTGGCCTGTTTGTT, SRB1 R: AGGATTCGGGTGTCATGAAG. HL F: TATGGCTGGAGGAATCTG, HL R: GCATCATCAGGAGAAAGG. LPL F: GTGGCCGAGAGCGAGAAC, LPL R: TCCACCTCCGTGTAAATCAAGA. LRP1 F:AGCATACCATCAACATCTC, LRP1 R: GTAGAGTTCCAGGTCCAG.

**Hepatocyte culture**

$8x10^6$ hepatocytes from high cholesterol diet-fed LDLR-/-G2A+/+ and LDLR-/-G2A-/- mice were plated at $10^6$/ml in serum-free Williams medium onto fibronectin-coated (10µg/well) 10cm tissue culture plates. 18 hours later, conditioned medium (16ml each from LDLR-/-G2A+/+ and LDLR-/-G2A-/- hepatocyte cultures) was collected and concentrated to 500µl using centrifugal filter devices (Amicon Ultra-15, 10K). Lipoproteins in concentrated conditioned media were separated by FPLC using a Superose-6 column as described above. Plasma from a control C57BL/6J mouse was separated to delineate HDL fractions in subsequent cholesterol profiles. Total cholesterol and phospholipid (Phospholipids C Kit, Wako, VA) content was measured in FPLC fractions from concentrated conditioned media and control plasma. HDL fractions were subjected to SDS-PAGE and immunoblotting for analysis of ApoA1 and ApoE levels.

**Statistics**

Statistical analysis was performed by the Mann Whitney Rank Sum test for aortic lesion coverage, aortic root lesion area, and lipoprotein concentrations using SigmaStat software. Statistical analysis of aortic lesion coverage, aortic root lesion area, and lipoprotein concentrations in the 4 groups of BM transplanted mice was performed by ANOVA. Pair-wise comparisons of aortic lesion coverage, aortic root lesion areas, and lipoprotein concentrations in the 4 groups of BM transplanted mice were performed by the Mann Whitney Rank Sum test. A $p$ value of less than 0.05 was considered significant.

**References**


1. Hedrick, C.C., Castellani, L.W., Warden, C.H., Puppione, D.L., and Lusis, A.J. 1993. Influence of mouse apolipoprotein A-II on plasma lipoproteins in transgenic mice. *J Biol Chem* 268:20676-20682.
2. Parks, B.W., Lusis, A.J., and Kabarowski, J.H. 2006. Loss of the Lysophosphatidylcholine Effector, G2A, Ameliorates Aortic Atherosclerosis in Low-Density Lipoprotein Receptor Knockout Mice. *Arterioscler Thromb Vasc Biol* 26:2703-2709.
3. Garber, D.W., Kulkarni, K.R., and Anantharamaiah, G.M. 2000. A sensitive and convenient method for lipoprotein profile analysis of individual mouse plasma samples. *J Lipid Res* 41:1020-1026.

**Supplemental Figure I (For publication online).** G2A deletion fails to raise plasma HDL in ApoE knockout mice. (**A**) Plasma concentrations of HDL-cholesterol and LDL-cholesterol in ApoE-/-G2A+/+ and ApoE-/-G2A-/- mice fed standard chow or high cholesterol (hi chol) diets for the indicated periods. (**B**) FPLC separation of plasma lipoproteins from high cholesterol diet-fed (20 weeks) ApoE-/-G2A+/+ and ApoE-/-G2A-/- mice. Inset: immunoblot of pooled consecutive pairs of HDL fractions indicated by dashed lines with an ApoA1-specific antibody. Note indistinguishable levels of ApoA1 immunoreactivity in HDL fractions from ApoE-/-G2A+/+ and ApoE-/-G2A-/- mice. 1: ApoE-/-G2A+/+, 2: ApoE-/-G2A-/-. (**C**) The absence of ApoE abolishes the ability of G2A deletion to raise plasma HDL in hypercholesterolemic LDLR-/- mice. FPLC separation of plasma lipoproteins from male high cholesterol diet-fed (20 weeks) ApoE-/-LDLR-/-G2A+/+ and ApoE-/-LDLR-/-G2A-/- mice. Plasma lipoprotein profile from male high cholesterol diet-fed (20 weeks) ApoE+/+LDLR+/+G2A+/+ (C57BL/6J) mice is shown to demonstrate the position of HDL fractions. Inset: Anti-ApoA1 immunoblot analysis of ApoA1 content in pooled consecutive pairs of HDL fractions indicated by dashed lines. 1: Control high cholesterol diet-fed (20 weeks) C57BL6J, 2: ApoE-/-LDLR-/-G2A+/+, 3: ApoE-/-LDLR-/-G2A-/-.

**Supplemental Figure II (For publication online).** G2A deficiency does not suppress atherosclerosis in ApoE-/- mice. (**A**) Quantification of aortic lesion coverage in high cholesterol diet-fed (20 weeks) male and female ApoE-/-G2A+/+ and ApoE-/-G2A-/- mice (●, ○: average, ⊤: standard deviation, for each experimental group).

Representative *en face* aorta specimens from high cholesterol diet-fed male ApoE-/-G2A+/+ and ApoE-/-G2A-/- mice are shown alongside. (**B**) Mean lesion areas per section throughout the aortic root in the indicated high cholesterol diet-fed (20 weeks) male and female mice (●, ○: average, ⊤: standard deviation, for each experimental group). (**C**) Representative Oil-red-O stained aortic root sections from male and female high cholesterol diet-fed ApoE-/-G2A+/+ and ApoE-/-G2A-/- mice. (**D**) Quantification of aortic lesion coverage (left panel) and mean lesion area at the aortic root (right panel) in 1 year-old male and female mice fed a standard chow diet (●, ○: average, ⊤: standard deviation, for each experimental group). * Statistically significant differences in % lesion coverage and aortic root lesion area determined by Mann Whitney Rank Sum test.

**Supplemental Figure III (For publication online).** G2A deficiency does not suppress atherosclerosis in ApoE-/-LDLR-/- mice. (**A**) Quantification of aortic lesion coverage in high cholesterol diet-fed (20 weeks) male ApoE-/-LDLR-/-G2A+/+ and ApoE-/-LDLR-/-G2A-/- triple mutant mice (●, ○: average, ⊤: standard deviation, for each experimental group). Representative *en face* aorta specimens from high cholesterol diet-fed male ApoE-/-LDLR-/-G2A+/+ and ApoE-/-LDLR-/-G2A-/- mice are shown alongside. (**B**) Mean lesion areas per section throughout the aortic root in high cholesterol diet-fed (20 weeks) male ApoE-/-LDLR-/-G2A+/+ and ApoE-/-LDLR-/-G2A-/- triple mutant mice (●, ○: average, ⊤: standard deviation, for each experimental group). Representative Oil-red-O stained aortic root sections from male ApoE-/-LDLR-/-G2A+/+ and ApoE-/-LDLR-/-G2A-/- mice are shown alongside.

**Supplemental Figure IV (For publication online).** Plasma LDL-cholesterol concentrations in chimeric LDLR-/- mice. No statistically significant differences in LDL-cholesterol levels between the 4 groups of BM transplanted mice were detected by ANOVA and Mann Whitney Rank Sum test.

**Supplemental Figure V (For publication online).** G2A deficiency in resident tissues is sufficient to increase plasma HDL ApoA1 content. FPLC separation of plasma lipoproteins from the indicated high cholesterol diet-fed (20 weeks) chimeric LDLR-/- mice. Inset: immunoblot of pooled consecutive pairs of HDL fractions from the indicated BMT groups with ApoA1-specific and ApoE-specific antibodies. Densitometric quantification of ApoA1 and ApoE immunoreactivity in HDL fractions is shown above. Note significantly increased levels of ApoA1 in HDL fractions from Ly5.1 LDLR-/-G2A-/- mice transplanted with Ly5.2 LDLR-/-G2A+/+ BM cells (BMT group 3) and Ly5.1 LDLR-/-G2A-/- mice transplanted with Ly5.2 LDLR-/-G2A-/- BM cells (BMT group 4).

**Supplemental Figure VI (For publication online).** Representative co-immunofluorescence staining of aortic root aorta sections from each of the 4 transplantation groups (1-4 as in Figure 4) demonstrating the origin of lesional macrophages (CD11b) in recipient LDLR-/- mice (Ly5.1) from donor bone marrow (Ly5.2). Note the absence of host-derived (Ly5.1) $CD11b^+$ macrophages in lesions (upper rows in each of the 4 panels). Red: $CD11b^+$ macrophages. Green: $Ly5.1^+$ or $Ly5.2^+$ cells.

Supplemental Figure I

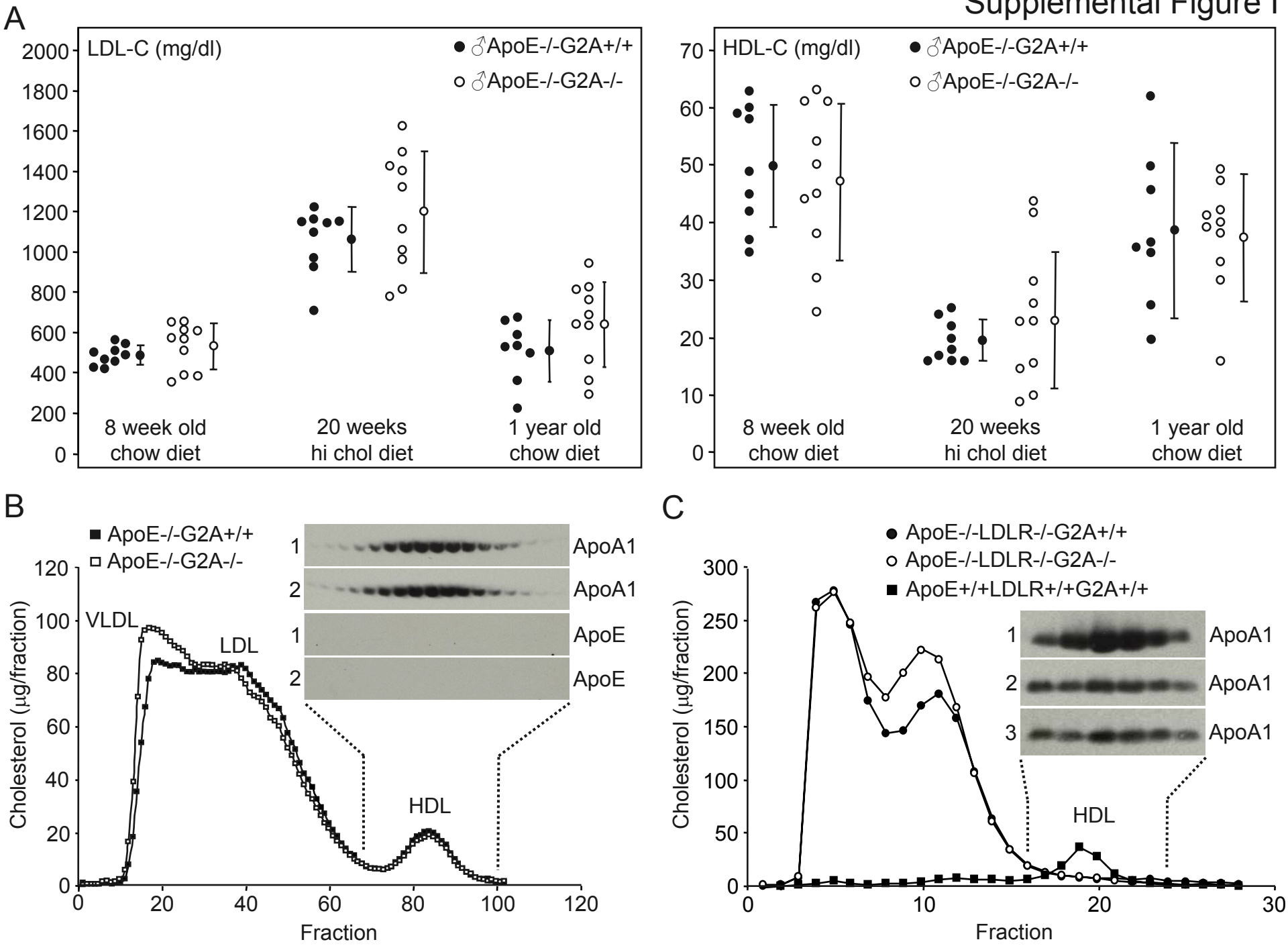

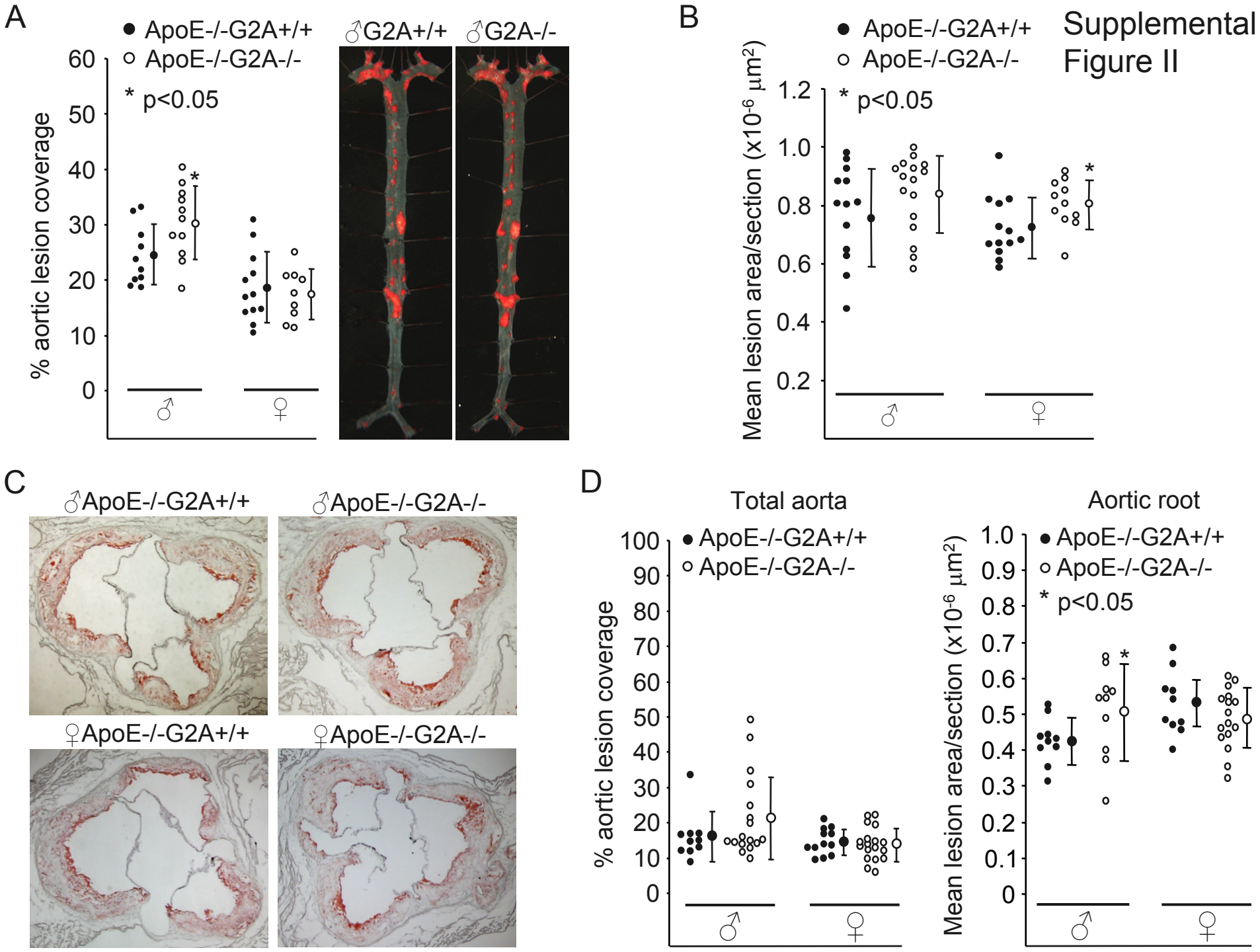
A
ApoE-/-G2A+/+
ApoE-/-G2A-/-
* p<0.05
% aortic lesion coverage
♂G2A+/+
♂G2A-/-
B
Supplemental Figure II
Mean lesion area/section (x10-6 µm2)
C
♂ApoE-/-G2A+/+
♂ApoE-/-G2A-/-
♀ApoE-/-G2A+/+
♀ApoE-/-G2A-/-
D
Total aorta
Aortic root

Supplemental Figure III

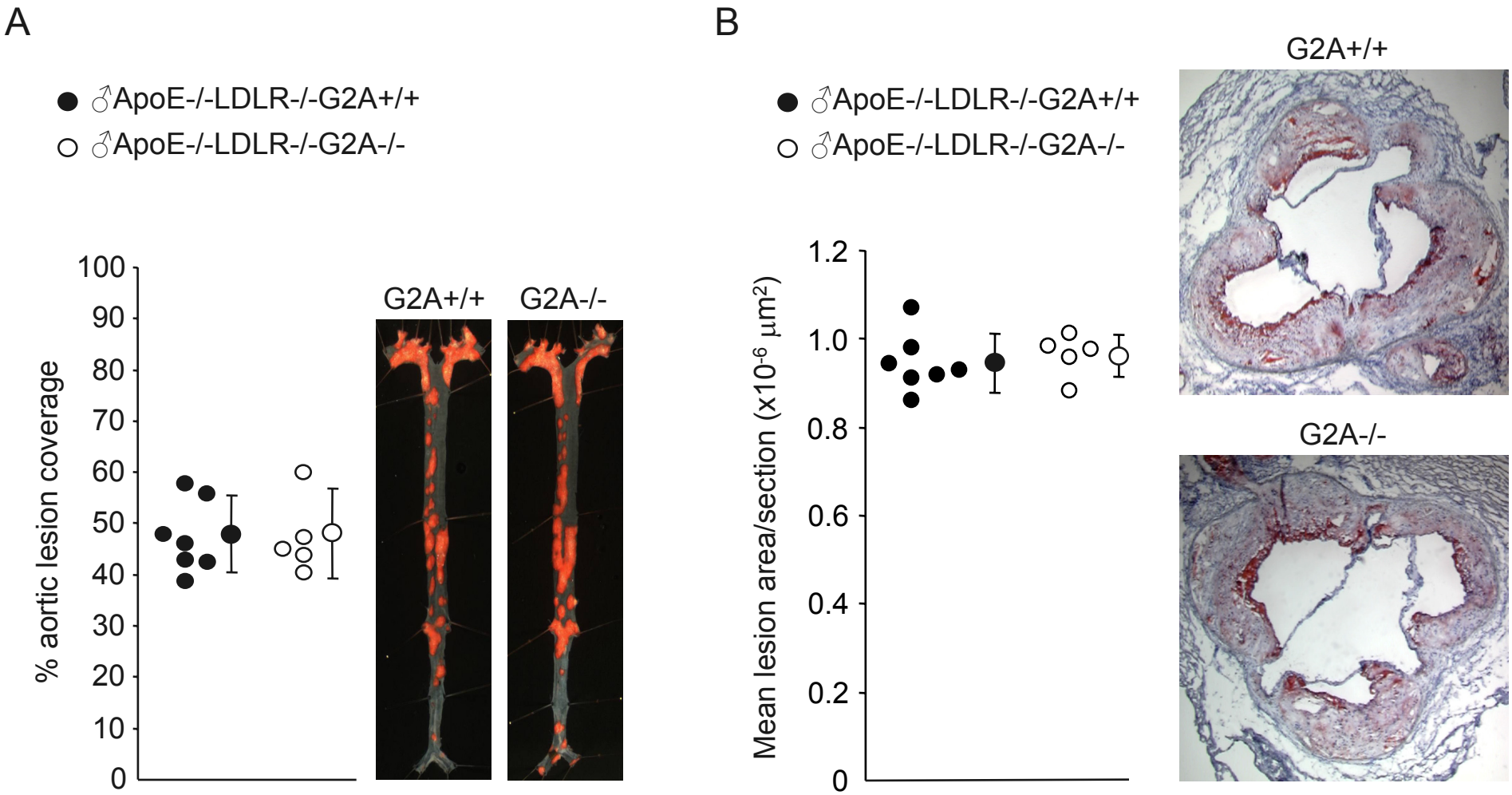

Supplemental Figure IV

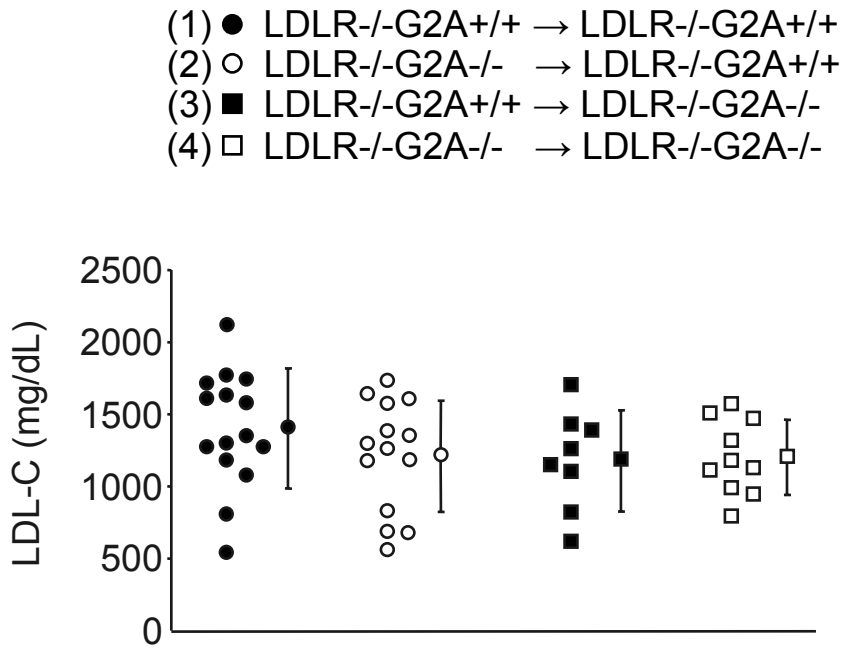

Supplemental Figure V

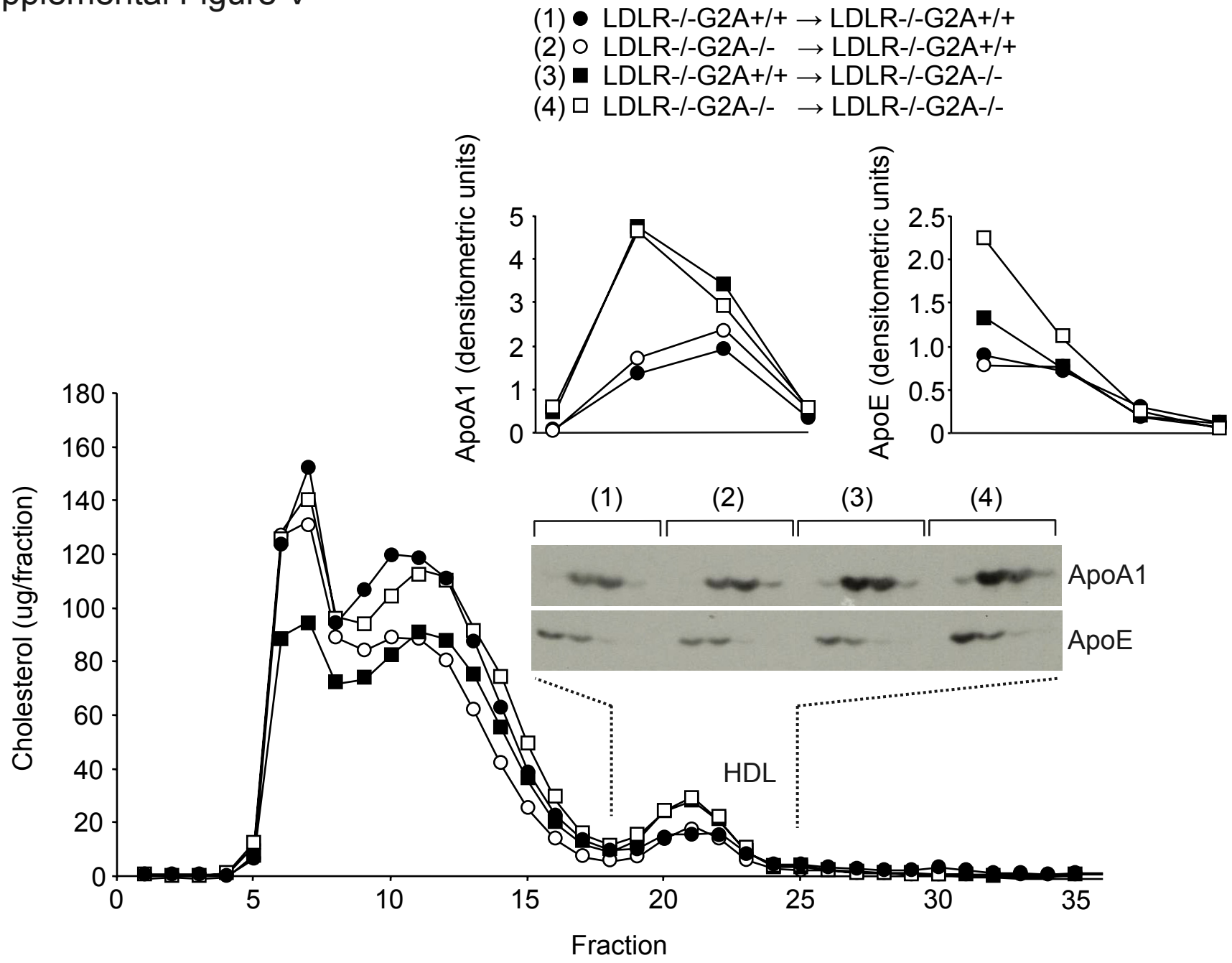

# Supplemental Figure VI

(1) Ly5.2 LDLR-/-G2A+/+ → Ly5.1 LDLR-/-G2A+/+

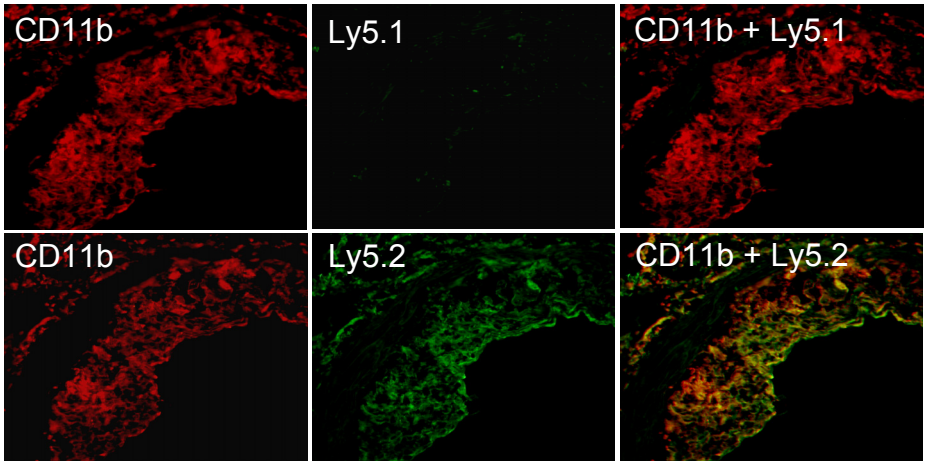


(2) Ly5.2 LDLR-/-G2A-/- → Ly5.1 LDLR-/-G2A+/+

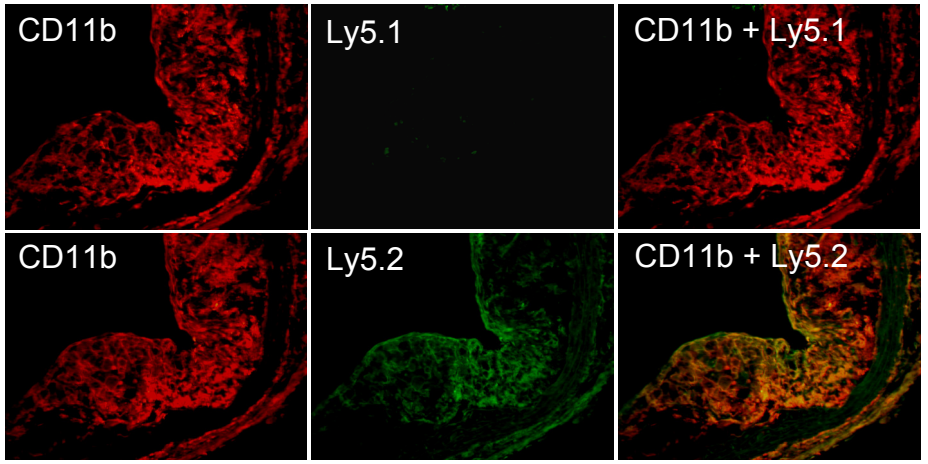


(3) Ly5.2 LDLR-/-G2A+/+ → Ly5.1 LDLR-/-G2A-/-

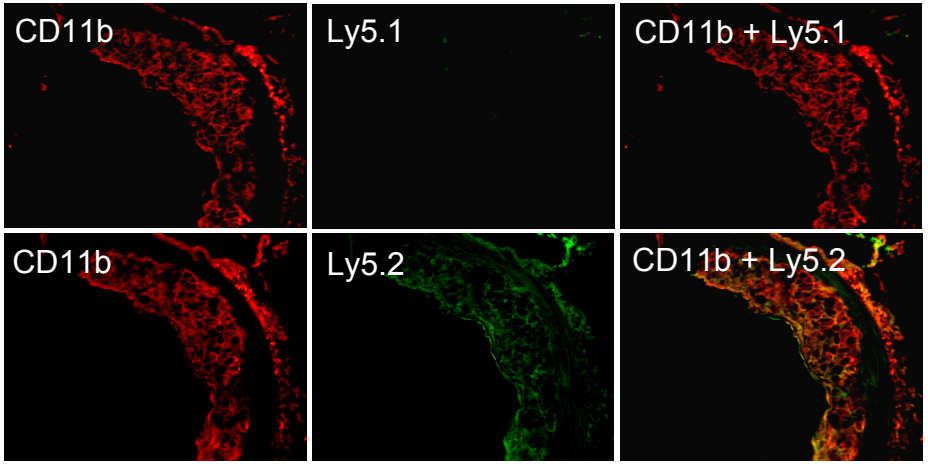


(4) Ly5.2 LDLR-/-G2A-/- → Ly5.1 LDLR-/-G2A-/-